Korean J. Chem. Eng., 32(7), 1229-1242 (2015)
DOI: 10.1007/s11814-014-0347-1

pISSN: 0256-1115
eISSN: 1975-7220

Design of a dividing wall column for fractionation of biodiesel

Hyun Jun Cho, Sung Ho Choi, Tae Young Kim, Jin-Kuk Kim, and Yeong-Koo Yeo†

Department of Chemical Engineering, Hanyang University, Haengdang-dong, Sungdong-gu, Seoul 133-791, Korea
(*Received 26 September 2014 • accepted 23 November 2014*)

Abstract−This study presents an efficient design method for DWC which can fractionate palm methyl esters (PME, biodiesel) into three more valuable product groups: a mixture of methyl laurate and methyl myristate as light-cut, pure methyl palmitate (≥99.5%) as middle cut, and the mixture of the remaining methyl esters (biodiesel), which has good low-temperature operability to such an extent as to come close to cold filter plugging point (CFPP) 0 °C, as heavy cut. The first step of the design was to determine numbers of stages for four sub-sections of DWC, liquid split ratio, and initial reflux ratio by the shortcut design, based on the component net flow model and the method of Fenske, Underwood, and Gilliland (FUG method). Secondly, optimal reflux ratio, vapor split ratio, locations of stages for feed and side product were found out by sensitivity analysis in rigorous simulation. The results from the simulation model developed by the method show that the reboiler duty of a single DWC is about 24% less than that of two simple columns in direct sequence and about 25% less than in indirect sequence. These energy saving ratios are almost close to 30%, which is popularly known as a typical value for energy saving of DWC.

Keywords: Dividing Wall Column, Palm Methyl Ester, Fractionation, Design, Cold Filter Plugging Point

INTRODUCTION

The use of palm methyl esters (PME) at high blend ratio and/or in geographical regions outside tropical latitudes is limited mainly due to poor operability in low temperature condition [1], although PME is currently one of the most popular biodiesels in the world. Low-temperature operability of biodiesel is normally determined by three common physical properties: cloud point (CP), pour point (PP), and cold filter plugging point (CFPP). The CFPP is the lowest temperature at which a given volume of biodiesel completely flows under vacuum through a wire mesh filter screen within 60 seconds. It is generally considered a more reliable indicator of low-temperature operability than CP or PP, since solids contained in the fuel are large enough to render the engine inoperable due to fuel filter plugging once the CFPP is reached [2]. The CFPP of PME, generally found to be 10-16 °C in the literature, is higher than that of soybean methyl esters (SME), −4 to −2 °C, and that of rapeseed methyl esters (RME), −14 to −9 °C. Poor CFPP property of PME is mainly related to the degree of unsaturation because PME has, typically, about 50% (w/w) of saturated components. Table 1 shows typical compositions and distributions of fatty acid methyl esters for three types of biodiesel. Having ~50% of saturated components for PME is considerably higher than SME (<12%) and RME (<16%) [2]. Main saturated component in PME is methyl palmitate ($C_{16:0}$), while other saturated components include methyl stearate ($C_{18:0}$, <5%) and saturated methyl esters of fewer carbon chains (<3%), for example, methyl myristate ($C_{14:0}$) and methyl laurate ($C_{12:0}$). Among these, the 'saturated methyl esters of fewer carbon chains' (the 1st group), i.e., methyl laurate and methyl myristate, are highly demanded materials in the oleochemical industry [3], produced mainly from coconut oil and palm kernel oil of which scarcity value is relatively higher than palm oil. Pure methyl palmitate (>99%), the second group, can be applied to the feedstock for fatty alcohol--cetyl alcohol--which is useful in the cosmetic industry [4] and/or in the oleochemical industry [5]. The mixture of the rest of methyl esters, the third group, excluding the above saturated methyl esters from

Table 1. Typical compositions and distributions of fatty acid methyl esters for three types of biodiesel

	$C_{14:0}$ [a]	$C_{16:0}$	$C_{18:0}$	$C_{20:0}$	$C_{22:0}$	$C_{18:1}$	$C_{18:2}$	$C_{18:3}$	ΣSats	ΣUnsats
PME (%)[b]	2.4	43.9	4.9	0	0	39.0	9.5	0.3	51.2	48.8
RME (%) [1]	0.3	4.3	1.4	2.1	3.9	54.5	16.1	16.1	12.0	88.0
SME (%) [1]	0.2	11.3	3.6	0.2	0.3	22.2	50.2	12.0	15.6	84.4

Note: In "$C_{m:n}$", "m" denotes the number of carbon atoms in the fatty acid chain, and "n" represents the number of double bonds in the chain
[a]The sum of compositions for methyl esters of fewer carbon chains, i.e. $C_{10:0}$, $C_{12:0}$ and $C_{14:0}$
[b]Analysis result by gas chromatography for a PME sample, provided by SK Chemicals Inc. in Korea

†To whom correspondence should be addressed.
E-mail: ykyeo@hanyang.ac.kr

PME, is also expected to have much improved CFPP property than PME. Therefore, there is strong economic incentive for the fractionation of PME into three groups: the 'saturated methyl esters of fewer carbon chains', the pure methyl palmitate, and the 'rest methyl esters', which allows simultaneous production of the higher value-added products, and the better biodiesel of the improved CFPP, compared to original PME.

On the other hand, there are a few works reported in the references for improving the low-temperature operability of PME, for example, blending with RME or SME which contains low saturated components [6-8] or addition of cold flow improvers as an additive to PME [1,6,9], while crystallization fractionation, widely known as winterization, has been widely practiced in industries, which exploits relative differences in melting points between components for removing the saturated components from PME [6,10]. Crystallization fractionation is effective for separating saturated methyl esters group from unsaturated methyl esters group; however it is limited to achieving sharp separation of methyl palmitate from the other saturated methyl esters, and hence to meet its specification as oleochemical feedstock. Another design option for the separation of methyl esters is fractional distillation, which has been applied in practice [11,12].

According to Heck et al. [11], the fractional distillation system to obtain a technical grade of methyl oleate ($C_{18:1}$), having methyl stearate ($C_{18:0}$) content of less than about 2% by weight, and methyl palmitate content of less than about 5%, should be composed of four simple columns in sequence. While the conventional distillation system allows sharp separation, this system inherently requires significant energy consumption. Therefore, it is sensible to investigate alternative separation systems for improving economic and environmental viability for PME separation. Among various technologies available, utilization of a dividing wall column (DWC) is considered in this study because DWC systems can achieve considerable energy savings, typically 30%, compared to conventional distillation systems using simple columns, without compromising product quality [13-21].

Therefore, the present study aims to provide an efficient method for the design of a single DWC which can fractionate PME into three products: the methyl esters of fewer carbon chains ($C_{12:0}$ & $C_{14:0}$) with methyl palmitate ($C_{16:0}$) content of less than 0.1%, as light-cut, the pure methyl palmitate (≥99.5%) as middle cut, and the rest of methyl esters (biodiesel) which have better CFPP, i.e. 0 °C, than PME as heavy cut. This design method presented in this paper consists of two major phases, which are relatively simple and less time-consuming in computation. The first is the application of short-cut design methods to determine numbers of stages for four sub-sections of DWC, liquid split ratio, and initial reflux ratio which are based on the component net flow model [22] and the method of Fenske, Underwood, and Gilliland (FUG method). Secondly, optimal reflux ratio, vapor split ratio, locations of stages for feed and side product were determined by sensitivity analysis using rigorous simulation. In the present work, the economic benefit of DWC for the fractionation of PME was also evaluated by the compari-

Table 2. The correlations for estimation of CFPP found in literatures

Source	Correlations	Effective range of ΣSats (wt%)	R^2
Gómez et al. [24]	CFPP (°C)=0.99*ΣSats−19.0	14-26	0.95
Moser [8]	CFPP=0.438*ΣSats−8.93	12-48.2	0.98
Park et al. [7]	CFPP=−0.4880*ΣUnsats+36.0548	12-100	N. A.
Ramos et al. [25]	CFPP=3.1417*LCSF(B)−16.477	N. A.	0.966
	where, LCSF(B)=0.1*$C_{16:0}$+0.5*$C_{18:0}$+1*$C_{20:0}$+1.5*$C_{22:0}$+2*$C_{24:0}$		

Note: $C_{m:n}$ - concentration (wt%) of 'component $C_{m:n}$'

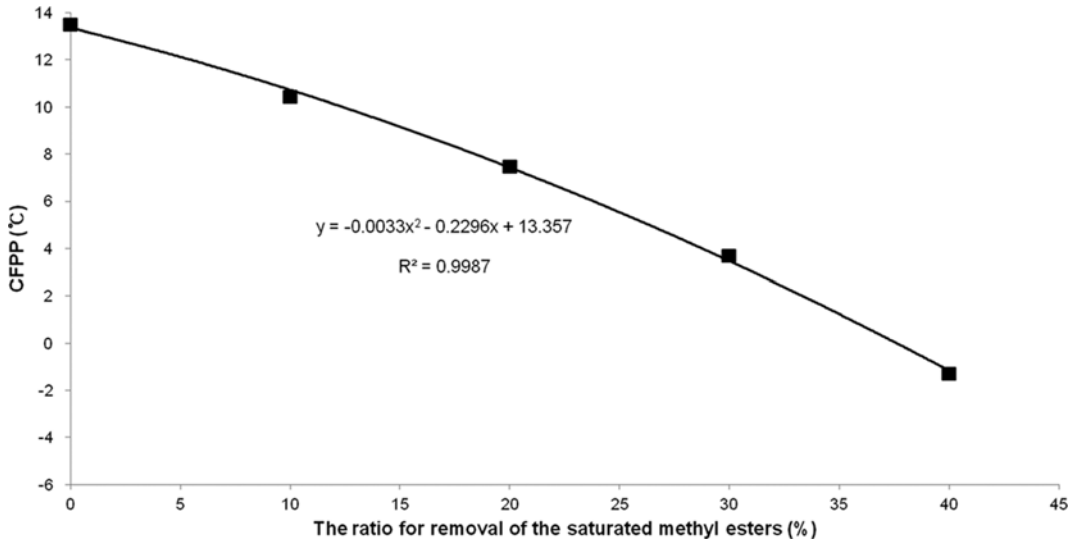

Fig. 1. A correlation of CFPP of the 'rest methyl esters' with the ratio for removal of the saturated methyl esters ($C_{12:0}$, $C_{14:0}$ & $C_{16:0}$).

son of the energy requirement with those of the conventional distillation systems which are composed of two simple columns in direct sequence and indirect sequence.

METHOD

1. Estimation of CFPP

The low-temperature operability of biodiesel may be estimated based on the concentration of total saturated methyl esters (Σ(Sats)) [23]. Some correlations, reported in the literature, for estimation of CFPP as a function of Σ(Sats) are shown in Table 2. The effective range of correlations and their accuracy in terms of coefficient of determination (R^2) were compared from the viewpoint of applicability for the composition of PME and 'rest methyl esters' group notated as the third group in this study, with which the correlation proposed by Moser et al. [8] was selected for estimating CFPP. A correlation to estimate CFPP of the 'rest methyl esters' as a function of the ratio for the removal of the saturated methyl esters, having carbon chains below 16, can be easily obtained based on the correlation of Moser et al. [8] as shown in Fig. 1. From the correlation in Fig. 1, the ratio for removal of the saturated methyl esters ($C_{12:0}$, $C_{14:0}$ and $C_{16:0}$), required to meet a target CFPP of the 'rest methyl esters', i.e., 0 °C in the present work, can be calculated.

2. Design of DWC

Design of the DWC is more complex than a simple column because there are more degrees of freedom to be specified. Key variables and parameters such as the distribution and number of plates in each of the column sections, reflux ratio, liquid and vapor splits to each side of the dividing wall, the feed stage locations and side-draw locations, must be established before simulation can be performed. These degrees of freedom all interact with each other and need to be optimized simultaneously to obtain the best design [26]. A common difficulty associated with the design of DWC is related to estimation of the number of stages in each column section. Since number of stages is an integer variable, the optimal design of DWC falls into a class of mixed integer non-linear programming problems (MINLP). This cannot be done within commercially available process simulators. To overcome this, usually an external optimization routine is introduced, coupled with process simulators [21]. But, the optimization-based methods [27-29] to solve these kinds of MILNP problems are reported to have extreme complexities in problem formulation and great difficulties in approaching the optimum solution [30].

To gain conceptual understanding in key design parameters for the design of distillation column, many researchers have proposed various 'short-cut design methods'. The works which considered the minimum vapor requirement as the most decisive factor for the design of DWC [31-33] paid less attention to the problem of determining the number of stages in the sub-sections of DWC [22]. Triantafyllou and Smith [34] applied the traditional shortcut method based on the Fenske, Underwood, and Gilliland equations to get the initial number of trays for each column. The operation leaves method based on the equilibrium stage composition concept by Amminudin et al. [26] also has the shortcomings in that they needed much time-consuming iterations and/or tunings to get solutions [22]. Although a structural design procedure by Kim [35] eliminates tedious iteration in calculation, this method was limited to carry out accurate determination of the number of the stages for sub-sections, because the number of trays was assumed to be equal to twice the minimum number of trays. Some statistical approaches such as 'factorial design' [15,16] and response surface methodology (RSM) [18,36-38] could be used with the aid of commercial software, and the predicted results by these approaches showed a good agreement with the actual trend from rigorous simulation. However, the design results from these methods can be significantly changed, depending on key variables selected and considered in the reduced model.

Recently, a novel shortcut method was reported that can be used to rapidly determine near-optimal values of important design parameters, including the reflux ratio, number of stages in all sections, and split liquid and vapor ratios. The method is based on the development of a rational and efficient net flow model and the application of the methods of Fenske, Underwood, and Gilliland (FUG) and the Kirkbride equation. The results show that this shortcut method leads to a process similar to a feasible actual process, and also provides good initial values for rigorous optimization [22]. However, because this shortcut is based on FUG method with the assumptions of constant relative volatility and constant molar internal flow, which is hardly the case in practice, direct implementation of these methods to the fractionation of PME must be avoided.

Therefore, in the present work, a two-staged method for the design of DWC for the fractionation of PME was proposed by methodologically integrating shortcut methods with rigorous simulation method, with which benefits of both design methods are fully exploited and shortcomings of each method are supplemented. Inaccuracy associated with taking assumptions of constant relative volatility and constant molar flow in shortcut methods is resolved by rigorous simulation by AspenPlus® (AspenTech, Inc.), while design difficulties in providing reliable and practical starting design points for DWC arrangement in rigorous simulation can be easily dealt with by relying on conceptual design information gained from shortcut methods. The first step of the design is to determine numbers of stages for four sub-sections, liquid split ratio and initial reflux ratio of DWC, which are the variables not easily determined by rigorous simulation, with the aid of short-cut method [22]. The second step is to screen key design parameters including reflux ratio, vapor split ratio, and locations of stages for feed and side product, and investigate their sensitivity in the economic performance, with which optimal design parameters for the DWC were determined.

2-1. Phase I: Short-cut Design

When the products should be fractionated into three groups by DWC, the first, named as product 'A', is the 'methyl esters of fewer carbon chains' ($C_{12:0}$ & $C_{14:0}$), the second, product 'B', is the pure methyl palmitate ($C_{16:0}$), and the third, product 'C', is the 'rest methyl esters' (biodiesel), as described in the introduction. For the convenience of calculation, product A can be represented by methyl myristate ($C_{14:0}$) and C by methyl oleate ($C_{18:1}$), because they have the closest boiling point to that of methyl palmitate ($C_{16:0}$), product B. Then, the changes of the relative volatilities of A and B with respect to C at 5 kPa, which were generated by AspenPlus®, can be shown as in Fig. 2. For ideal mixtures, a geometric average of the relativities for the highest temperature and lowest temperature in the col-

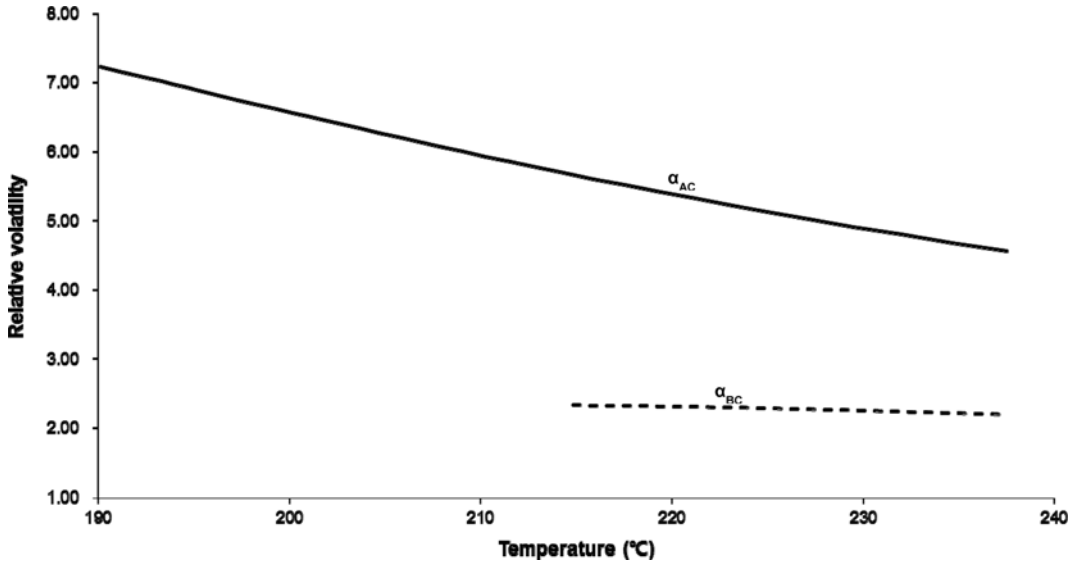

Fig. 2. The changes of the relative volatilities of A and B with respect to C at 5 kPa.

Table 3. Feed conditions and product specifications for the design of DWC in the present work

Feed		Product	
Flowrate (F)	100 kgmol/h	Top product composition (molar)	$X_{D2,A}/X_{D2,B}/X_{D2,C}=0.999/0.001/10^{-6}$
Quality (q)	1 (saturated liquid)	Side product composition (molar)	$X_{S,A}/X_{S,B}/X_{S,C}=0.001/0.995/0.004$
Composition (molar)	$Z_A/Z_B/Z_C=0.028/0.459/0.513$	Bottom product composition (molar)	$X_{W4,A}/X_{W4,B}/X_{W4,C}=10^{-6}/0.165/0.835$
Relative volatility	$\alpha_{AC}/\alpha_{BC}/\alpha_{CC}=5.745/2.261/1.000$		

umn usually gives sufficient accuracy in the computations [39], and the average, $\alpha_{ij,avg}$, can be calculated by Eq. (1).

$$\alpha_{ij,avg}=\sqrt{\alpha_{ij,top}\times\alpha_{ij,bot}} \quad (1)$$

where, $\alpha_{ij,top}$ and $\alpha_{ij,bot}$ are the relative volatilities at top and bottom of column, respectively. Therefore, the average volatilities of A and B with respect to C can be obtained from Fig. 2 and Eq. (1). In a commercial plant, feed is usually given as liquid and the feed composition of PME can be assumed to be same as in Table 1. Considering the product specification described in the introduction (section 1) and the target ratio for the removal of the saturated methyl esters from Fig. 1, which enables the CFPP of the 'rest methyl esters' to be 0 °C, basic information needed for the design of DWC can be simplified and summarized as shown in Table 3.

The DWC in the present study is divided into five sections as shown in Fig. 3. Section 1 corresponds to the pre-fractionator. Section 2 is a rectifying section and section 4 is a stripping section. Section 3_1 is the upper section on the right side of the dividing wall, and section 3_2 is the lower section on the right side of the dividing wall. The component net flow model proposed by Chu et al. [22] has been adopted for the short-cut calculation for DWC in this study, because their short-cut method is effective to determine rapidly near-optimal values of key design parameters for DWCs. According to Chu et al. [22], the component net flow model has two assumptions that the net flow of C at the top of section 1 is equal to the flow of C in the side-draw, and that the net flow of A at the bottom of section 1 is equal to the flow of A in the side-draw,

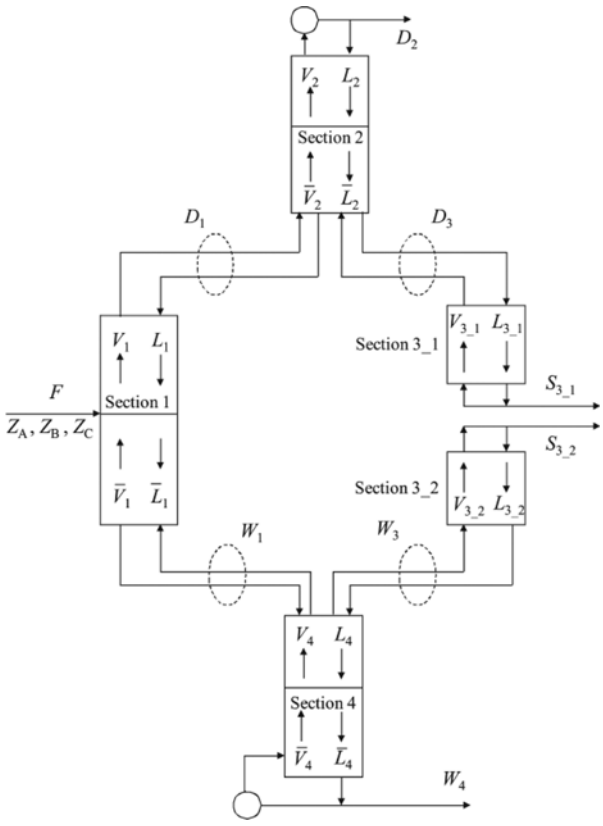

Fig. 3. A schematic diagram for DWC by Chu et al. [22].

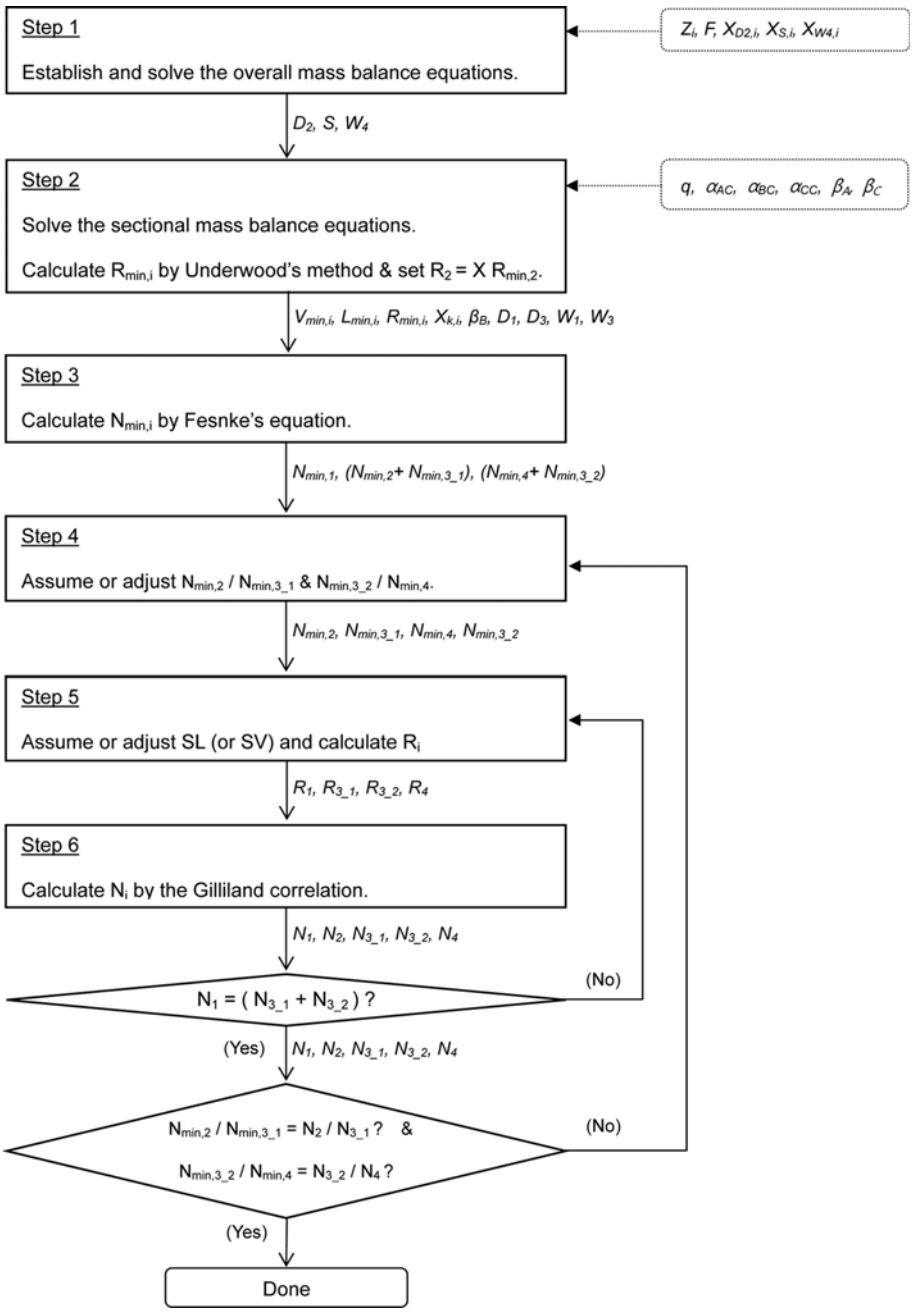

Fig. 4. The procedure for the shortcut design of DWC in this work based on Chu et al. [22].

avoiding the 'long way around travel'. These assumptions allow the engineer to determine approximate values of the composition at key points in the column if the feed flow rate, feed composition, and product specifications are known. Overviews for the short-cut method of Chu et al. [22] can be found in the appendix, which describes a design parameter, β_i, representing the fraction of i sent to the top of the pre-fractionator[1], a calculation procedure for estimating the minimum vapor flow rate in each column section, and a design method for obtaining minimum reflux ratio and minimum number of stages. The overall procedure for the shortcut design in the present work is summarized as shown in Fig. 4.

A different number of stages between section 1 and section 3 may be considered for detailed design as long as the difference is not too practically large to be implemented. However, we believe that the same number of stages is a reasonable and practical engineering decision in the conceptual design stage, because advantages obtained from different number of stages cannot be fully judged before studying detailed column sizing and column hydraulic performance.

2-2. Phase II: Rigorous Simulation

Most of studies for the shortcut design of DWC, including that of the present work, have been based on FUG methods or at least

[1]In this study, 0.999 and 0.001 were used for β_A and β_C.

on Fenske's equation or on Underwood's method. As discussed earlier, the basic assumptions related with these methods, constant molar flow' and/or constant relative volatility, may be the main obstacles to applying the shortcut design to actual plant. Nevertheless, the values for the key design parameters, obtained by the shortcut method in the present work, are very meaningful because these values are close to optimal ones studied by Chu et al. [22]. Especially, the numbers of stages in all subsections, which have not been determined easily with acceptable tolerance by other studies, and the split ratio (SL or SV), which was determined in order to assure the same numbers of stages on both sides of the dividing wall (N_1= N_3), from the shortcut design in the present work can be informative enough to be directly used for rigorous simulation. Once the values for these key design parameters are obtained, the optimization is carried out for determining the other design parameters without having any computational difficulties or convergence issues, with the aid of sensitivity analysis tool available in AspenPlus®.

The first thing to do in rigorous simulation is to check whether the product specifications are met with the design parameters from the shortcut design, or not. If any product composition does not meet the target purity, the reflux ratio (R_2) should be increased until the composition reach the target with the number of stages in each subsection and the liquid split ratio (SL) kept same as the shortcut design. Of course, there could be the opposite case if the composition overpasses the specification. At the optimal reflux ratio found, the vapor split ratio (SV) and the locations of feed and side-product can be determined to minimize the reboiler duty of DWC. On the contrary to the shortcut design, SV does not depend on SL in the rigorous simulation because the constant molar flow assumption is not effective any more. The efforts to obtain the optimal values in rigorous simulation of the present work are drastically reduced due to the decrease in degree of freedom for design parameters and in the variance of the parameters. The optimal values for the reflux ratio and the vapor split are found during the adjustment to meet the product specifications and/or to minimize the reboiler duty, using the function of 'DesignSpec' or 'Sensitivity analysis' in AspenPlus®. And it does not require many trials to compute the optimal locations for feed and side-product because the variance of these parameters are limited within the numbers of stages for section 1 and section 3 which were already determined by the shortcut design. As a result, the rigorous simulation incorporated with the shortcut design in this work can lead to cost-effective and practical engineering solutions using relatively much less computational efforts and resources.

The original built-in physical property data were used for methyl myristate (C14:0), methyl palmitate (C16:0) and methyl oleate (C18:1), and the Soave-Redlich-Kwong (SRK) method as the equations of state for VLE calculation were selected for the rigorous simulation, because these methyl esters can be considered as non-polar components. Generally, DWC can be represented by two ways in AspenPlus® without any conflict over the concept of DWC, i.e., fully thermally heat-integrated distillation column. One is that DWC consists of two serial RadFrac columns, while a single MultiFrac column can be used in the other case. In the present work, the former was adopted, having the DWC composed of a pre-fractionator and a main column as shown in Fig. 5.

2-3. References: Conventional Distillation Systems

As is well known, considering separation of a three component

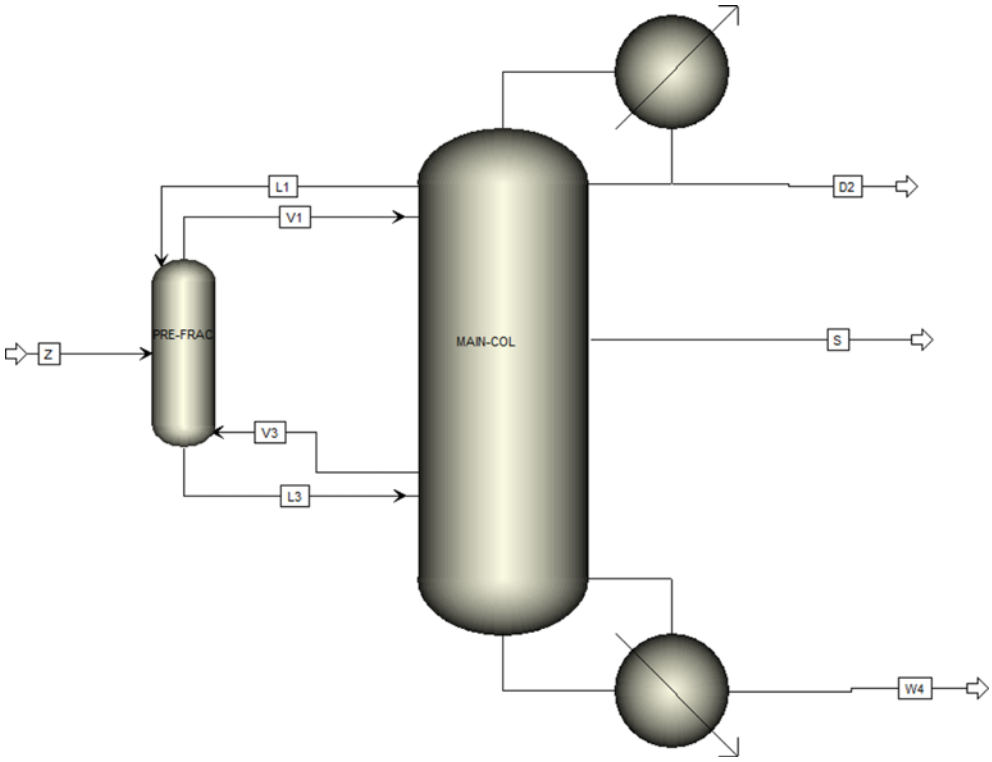

Fig. 5. The flowsheet for the DWC in the rigorous simulation of the present work.

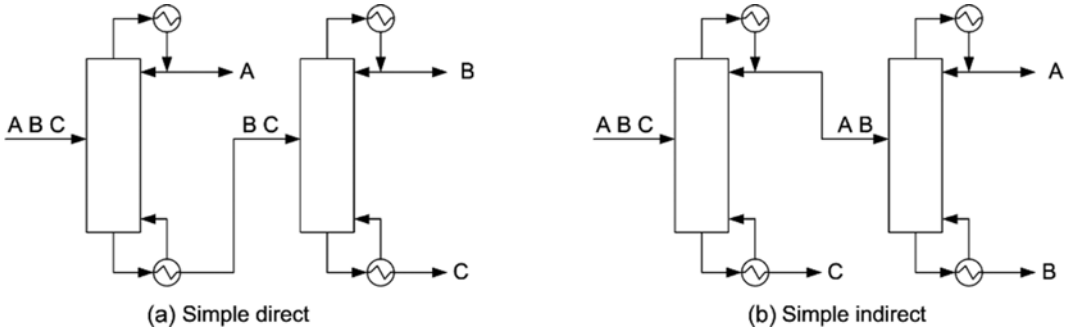

Fig. 6. Conventional arrangements of distillation columns for three component separation [21].

Table 4. The product specifications for the columns in conventional arrangements

	Direct (Fig. 6(a))	Indirect (Fig. 6(b))
1st Column	Top product composition (molar), $X_{top,A}/X_{top,B}/X_{top,C}$=0.999/0.001/$10^{-6}$ Recovery to top product (molar), β_A/β_B=0.98712/0.00006	Bottom product composition (molar), $X_{bot,A}/X_{bot,B}/X_{bot,C}$=$10^{-6}$/0.165/0.835 Recovery to top product (molar), β_B/β_C=0.77977/0.00280
2nd Column	Top product composition (molar), $X_{top,A}/X_{top,B}/X_{top,C}$=0.001/0.995/0.004 Bottom product composition (molar), $X_{bot,A}/X_{bot,B}/X_{bot,C}$=$10^{-6}$/0.165/0.835 Recovery to top product (molar), β_B/β_C=0.77975/0.00280	Top product composition (molar), $X_{top,A}/X_{top,B}/X_{top,C}$=0.999/0.001/$10^{-6}$ Bottom product composition (molar), $X_{bot,A}/X_{bot,B}/X_{bot,C}$=0.001/0.995/0.004 Recovery to top product (molar), β_A/β_B=0.98714/0.00008

feed into pure products, an obvious choice is to employ either the so-called direct or indirect configuration, shown schematically in Fig. 6(a) and (b), respectively [21]. To compare energy consumptions in the same basis, a two-phase method used for the design of DWC was applied for that of distillation columns in conventional arrangement. So, a shortcut design based on FUG method was first performed to find the number of stages in each column, followed by rigorous simulation to obtain optimal reflux ratio and locations for feed and side-product. The product specifications for each column in conventional arrangements are shown in Table 4. On the contrary to DWC, the parameters for the shortcut design in conventional systems can be readily obtained by FUG method and the rigorous simulation also needs less effort due to much fewer degrees of freedom. The results from the rigorous simulation will be compared to those of DWC to prove the validity of DWC. Considering capital cost, for example, TAC (total annualized cost) for economic evaluation would be preferred as long as accurate estimation for DWC can be made. However, due to lack of detailed and reliable costing data available for DWC, reboiler duty was chosen as a performance indicator in this study, which can be easily calculated from a simulation model and is not based on any engineering judgment or preference made in the application of costing data, for example, materials, site conditions, equipment types, etc.

RESULTS AND DISCUSSION

In the shortcut design of the present study, the optimal value for β_B, i.e., $\beta_{B,O}$, has to be found during the calculation of minimum vapor flow to obtain the values for the net internal flows (D_1, D_3, W_1, W_3) and the compositions in the net internal flows ($X_{k,j}$, k=1, 3, j=A, B, C) as well as the minimum reflux ratio of the DWC ($R_{min,2}$) after solving the overall mass balance equations. The value $\beta_{B,O}$, 0.6268, was determined in order that $V_{min,3\_1}$ can be equal to $V_{min,3\_2}$ and that $V_{min,DWC}$ can be minimum as shown in Fig. 7, bearing in mind that side-product should be withdrawn as liquid in actual plant. The values for the net internal flows, the compositions in the net internal flows, and the minimum reflux ratio of the DWC based on $\beta_{B,O}$ are shown in Table 5. The results for the minimum stages for section 1, section 2+section 3_1 and section 3_2+section 4 are also shown in Table 5, which were calculated by Eqs. (A8)-(A10). As a next step in the shortcut design, the number of stages in each section according to a certain reflux ratio, $1.2R_{min,2}$ in this work, was determined by adjusting the split ratio (SL), $N_{min,2}/N_{min,3\_1}$ and $N_{min,3\_2}/N_{min,4}$. Fig. 8 shows that the number of stages in section 1, N_1, is equal to that in section 3 (section 3_1+section 3_2), N_3, and that the numbers of stages on both sides of dividing wall section reach the minimum at the point of the optimal SL. Finally, the design results for the DWC in the present work are shown in Table 5.

The rigorous simulation model was developed, based on the design data from the shortcut method as shown in Table 5, using Aspen-Plus®. Considering the numbers of stages, 5.3 kPa and 2.4 kPa were applied as pressure drops for the main column and the pre-fractionator, respectively, with top pressures set to 5.0 kPa, 6.0 kPa, respectively. First, the product purities at the pre-determined values for reflux ratio, SL and the number of stages in all subsections and at

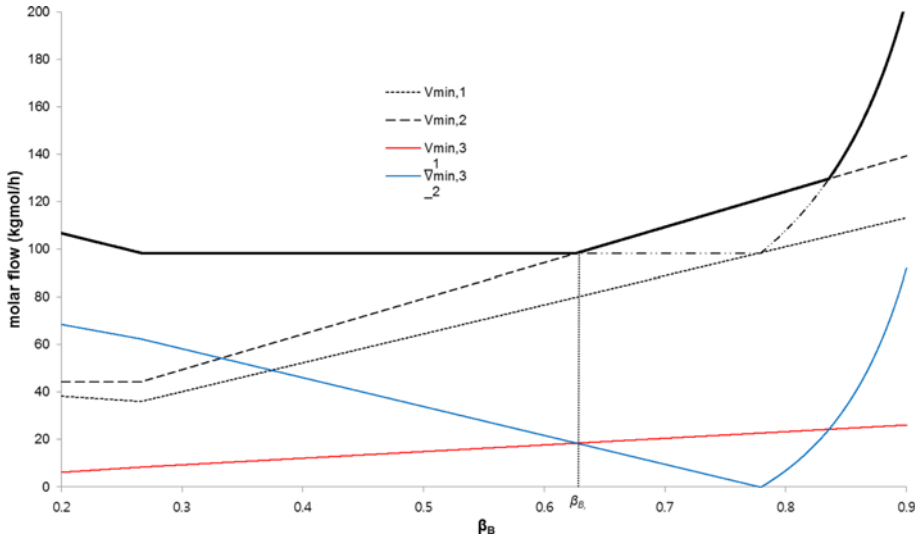

Fig. 7. The minimum vapor flows for each section and the DWC by the shortcut design in the present work.

Table 5. The results for the DWC by shortcut design of the present work

Design variables and parameters	Values
Product flows (kgmol/h)	$D_2/S/W_4$=2.77/35.97/61.26
Net internal flows (kgmol/h)	$D_1/D_3/W_3/W_4$=31.62/28.85/68.38/7.12
Compositions in the net internal flows (mole fraction)	$X_{A,D1}/X_{B,D1}/X_{C,D1}$=0.0885/0.9099/0.0016
	$X_{A,D3}/X_{B,D3}/X_{C,D3}$=0.0012/0.9970/0.0018
	$X_{A,W1}/X_{B,W1}/X_{C,W1}$=4*10^{-5}/0.2505/0.7495
	$X_{A,W3}/X_{B,W3}/X_{C,W3}$=0.0004/0.9866/0.013
Minimum reflux ratio for the DWC ($R_{min,2}$)	34.54
Minimum number of stages	$N_{min,1}$: 9.1
	$N_{min,2}+N_{min,3\_1}$: 14.7
	$N_{min,3\_2}+N_{min,4}$: 7.3
Other design parameters	R_2 : 41.44 (1.2$R_{min,2}$)
	SL : 0.483 (SV : 0.741)
	$N_1/N_2/N_3/N_4$=23/10/23/18

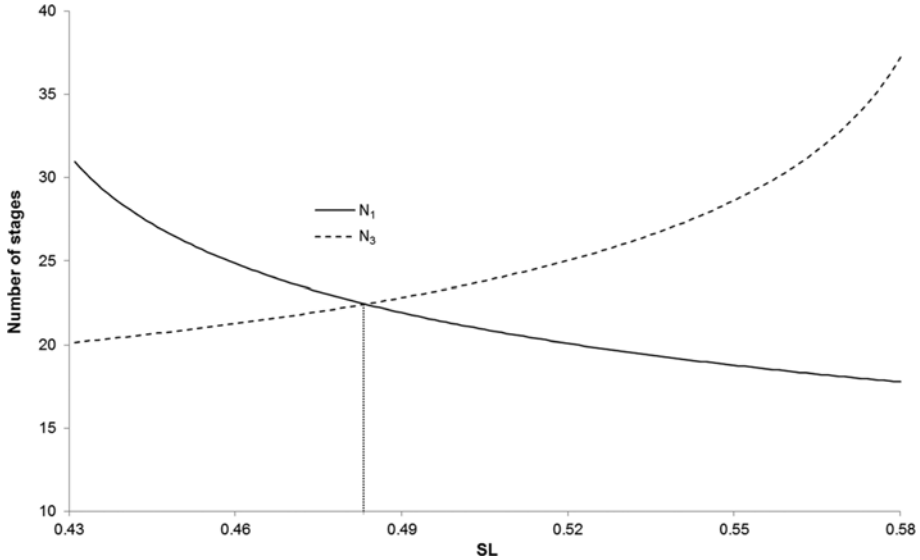

Fig. 8. Determination of number of stages in section 1 (N_1) and section 3 (N_3) at the optimal SL.

Table 6. The results from the sensitivity analysis in the rigorous simulation for DWC

Reflux ratio (R_2)	SV	Optimal location		Product purity (mole frac.)		
		Feed (N_F)	Side-product (N_{SP})	$X_{D2,A}$	$X_{S,B}$	$X_{W4,C}$
$1.2R_{min,2}$	0.60	10	28	1.000	0.845	0.747
	0.67	15	26	1.000	0.905	0.782
	0.74	6	29	0.999	0.924	0.793
$1.3R_{min,2}$	0.60	13	27	1.000	0.876	0.765
	0.67	16	23	0.999	0.940	0.803
	0.74	4	28	0.999	0.919	0.790
$1.4R_{min,2}$	0.60	15	28	0.999	0.903	0.781
	0.67	16	22	0.999	0.972	0.822
	0.74	4	30	0.999	0.913	0.787
$1.5R_{min,2}$	0.60	16	24	0.999	0.934	0.799
	0.67	13	20	0.999	0.994	0.834
	0.68[a]	**13**	**21**	**0.999**	**0.996**	**0.835**
	0.74	3	30	0.999	0.899	0.779

[a]The optimal point found in the sensitivity analysis

the changing values for SV, feed position (N_F) and side-product position (N_{SP}) were checked as to whether the product specifications were met or not. At the reflux ratio, SL, and the number of stages in all subsections as shown in Table 5, it was observed that any combinations of SV, N_F, and N_{SP} could not meet the product specifications. The optimal point, the best combination of N_F, N_{SP}, and SV, which enable to meet the given product specifications and to lead to minimum reboiler duty, were barely found when the reflux ratio reached $1.5R_{min,2}$ as shown in Table 6. In conclusion, the optimal values for the reflux ratio ($1.5R_{min,2}$) and the vapor split ratio (0.68) in the rigorous simulation are somewhat different from the values from the shortcut design ($1.2R_{min,2}$/0.741).

Such difference resulted from smaller internal flowrate (L_k) below the range of $1.5R_{min,2}$ in rigorous simulation than internal flowrate ($1.2L_{min,k}$) at $1.2R_{min,2}$ in shortcut design, which can be observed in Fig. 9. One of reasons for such difference in internal flowrates between shortcut design and rigorous simulation is that the heat balance is not considered in the shortcut design method adopted in this study, while it can be attributed that an underlying assumption of constant relative volatility for the shortcut model is not thoroughly valid for components A and C, as shown in Fig. 2. However, the assumption of constant molar flow for the shortcut seems to be reasonable for design purpose, which is illustrated in Fig 9.

SL and SV strongly affect heat duty and/or product purities, and hence they are important design parameters for DWC in practice. Rigorous simulation was carried out in this study to understand impacts of SL and SV on heat duty and product purities. As shown in Table 6, at fixed reflux ratio ($1.5R_{min,2}$), feed stage (N_F=13) and side-product stage (N_S=21), SL and SV have little impact on heat duty, as the reflux ratio is a main design variable for heat duty, while product purities are heavily dependent on the choice of SL and SV, and even off-specification products are produced for some operating range of SV and SL. A feasible design range for SL and SV to meet product specifications was determined through rigorous simulation, of which results are given in Fig. 10.

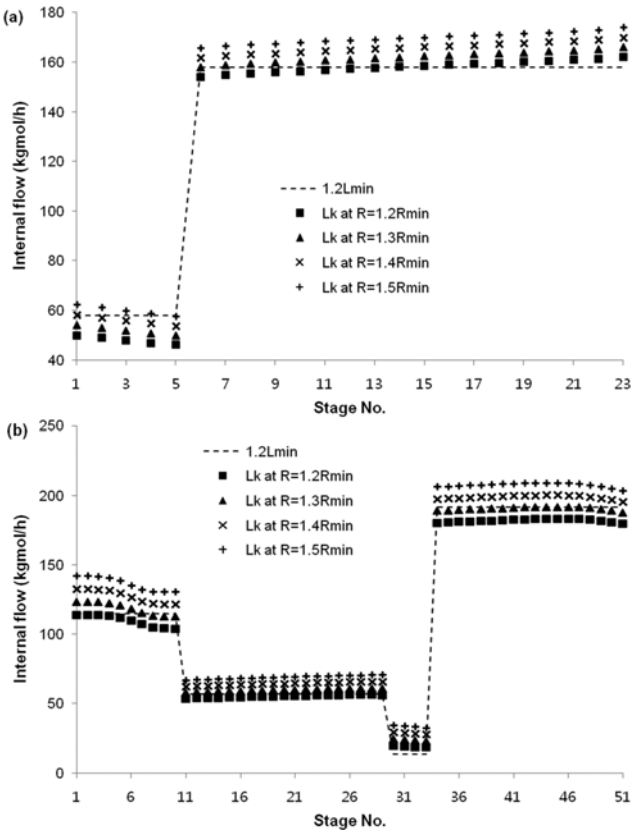

Fig. 9. The internal flow profiles for (a) the pre-fractionator and (b) the main column from the rigorous simulation of the present work.

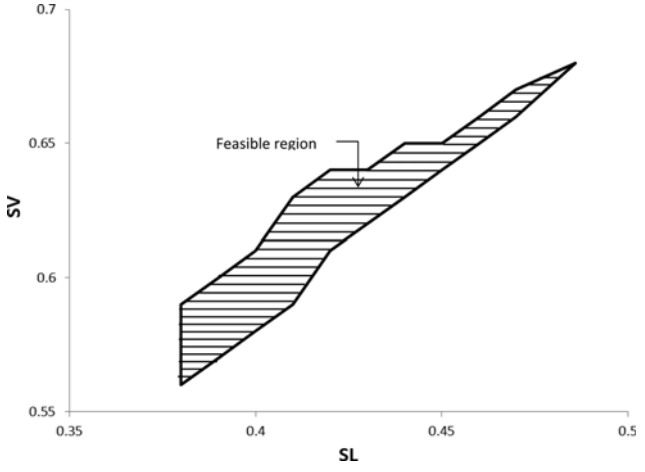

Fig. 10. A feasible region for SL an SV which enable the product specifications to be met in the present work ($R=1.5R_{min,2}$, N_F=13, N_S=21).

Overall, it is reasonable that most shortcut methods for DWC, which are based on FUG method, may be inaccurate or infeasible, if directly applied to an actual plant. Therefore, it is preferable

Table 7. The design results for the columns in the conventional arrangements by FUG method

Sequence		Direct (Fig. 6(a))	Indirect (Fig. 6(b))
1st Column	Minimum reflux ratio ($R_{min, col1}$)	14.89	1.56
	Minimum number of stages	16.74	8.91
	Number of stages at $R=1.2R_{min, col1}$	31.14	18.36
2nd Column	Minimum reflux ratio ($R_{min, col2}$)	1.81	9.37
	Minimum number of stages	8.92	16.31
	Number of stages at $R=1.2R_{min, col2}$	18.15	30.52

Table 8. The results from the sensitivity analysis in the rigorous simulation for the conventional arrangements

Sequence	Column	Reflux ratio	Feed location (N_F)	Product purity (mole frac.)		
				$X_{prod, A}$	$X_{prod, B}$	$X_{prod, C}$
Direct	1st Column	$1.2R_{min, col1}$	12	0.949	-	-
		$1.5R_{min, col1}$	13	0.995	-	-
		$1.63R_{min, col1}$[a]	**14**	**0.999**	-	-
	2nd Column	$1.2R_{min, col2}$	12	-	0.966	0.818
		$1.45R_{min, col2}$[a]	**15**	-	**0.995**	**0.835**
Indirect	1st Column	$1.2R_{min, col1}$	10	-	-	0.814
		$1.5R_{min, col1}$	13	-	-	0.832
		$1.67R_{min, col1}$[a]	**15**	-	-	**0.835**
	2nd Column	$1.2R_{min, col2}$	11	0.963	0.993	-
		$1.5R_{min, col2}$	12	0.997	0.995	-
		$1.62R_{min, col2}$[a]	**14**	**0.999**	**0.995**	-

[a]The optimal point found in the sensitivity analysis

that the final design results for DWC have to be obtained only from the rigorous simulation, like this work.

As a reference work, the design for distillation columns in conventional arrangements was also performed in this study. The shortcut design results for the columns to meet the specifications in Table 4, based on the FUG method, are shown in Table 7. The results for the sensitivity analysis in the rigorous simulation are presented in Table 8, which shows that the product specifications cannot be met by the product purities using the reflux ratio and the number of stages in each column, which were determined by FUG method, and that the optimal point in each column can be found on an increased reflux ratio, as like the results for the DWC. These gaps are also considered to originate from the assumptions made in the FUG method.

The design results for the fractionation systems by the DWC and by the conventional arrangements are summarized as Fig. 11. From the results, the reboiler duty for the DWC is about 24% less than that of two series columns in direct sequence and about 25% less than in indirect sequence. This kind of energy reduction by DWC is attributed to the removal of inefficiency in conventional arrangements. According to Triantafyllou and Smith [34], the inefficiency in conventional arrangements comes from the remixing of the middle component (B) and from the remixing on the feed stage due to the discrepancy between the feed composition and the composition on the feed plate. There is no remixing of the component B found in the profiles for DWC of the present work, whereas some inevitable mismatches between the feed composition and the composition on the feed stage were detected (Fig. 12). On the other hand, the two-phased design method in the present work was not proven to be perfect for the design of DWC, considering a slight decrease in the composition of B in top section of fractionator, as shown in Fig. 12. This phenomenon was related to compositional mismatches between inter-connecting sections, e.g., between the composition in the top of pre-fractionator and the composition in the bottom of section 2, as shown in Fig. 13(a). This inconsistency was easily remedied by moving the location of the dividing wall section down to five stages, by increasing five stages for the number of stages in section 2 and by decreasing five stages for the number of stages in section 4, keeping the number of stages in both sides of dividing wall section the same as the original design. After the adjustment of the number of stages, the mismatches were almost alleviated as shown in Fig. 13(b) and that the reboiler duty was reduced to 10.620 GJ/hr, which is about 26% less than that of two series columns in direct sequence and about 27% less than in indirect sequence. Only about 2% was improved by the adjustment of the number of stages, compared to the original design.

CONCLUSION

We have presented an efficient design method for DWC which can fractionate PME into three more valuable product groups--a mixture of methyl laurate and methyl myristate as light-cut, pure

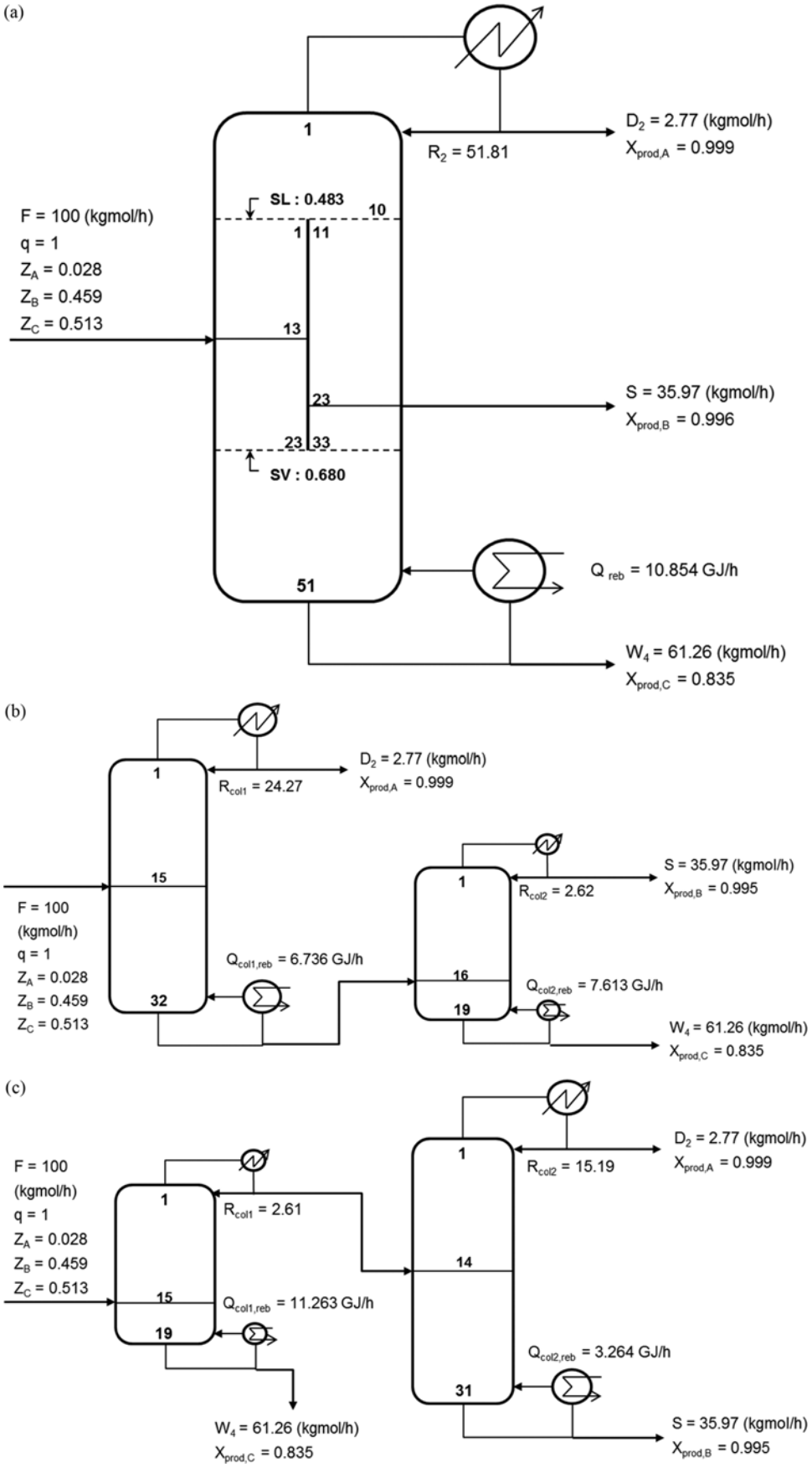

Fig. 11. The design results for the fractionation systems by (a) DWC, (b) direct sequence and (c) indirect sequence in conventional arrangement.

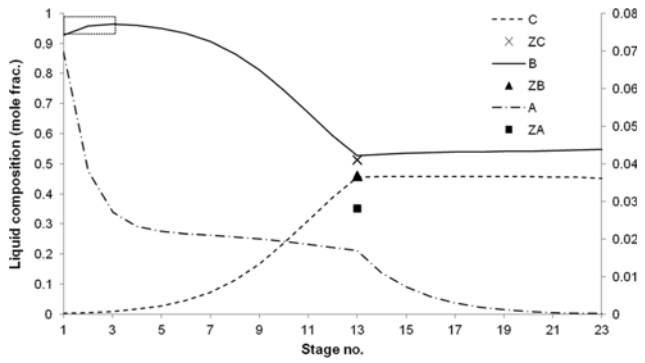

Fig. 12. The composition profiles for the pre-fractionator of DWC in the present work.

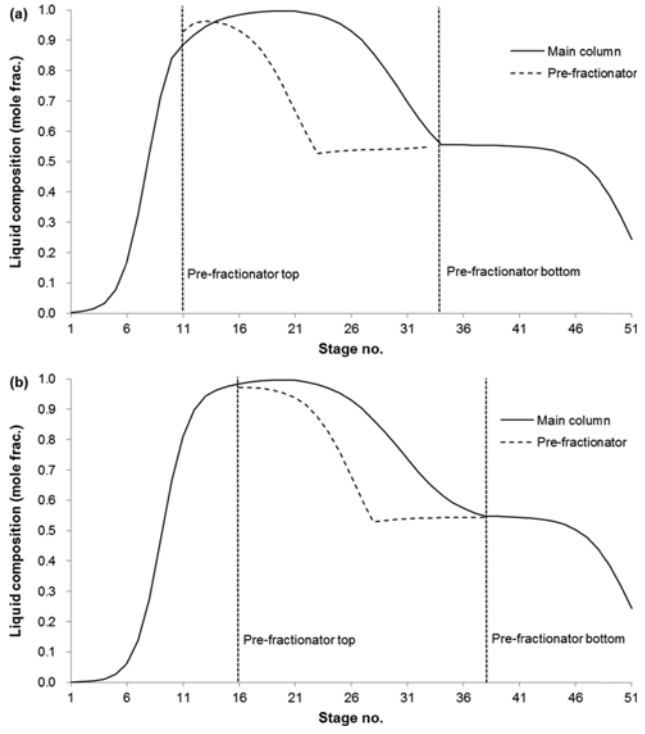

Fig. 13. The composition profiles for component B in the DWC (a) before the adjustment of the number of stages (b) after the adjustment of the number of stages.

methyl palmitate (≥99.5%) as middle cut, and the mixture of the remaining methyl esters (biodiesel)--which has the good low-temperature operability to such an extent as to come close to cold filter plugging point (CFPP) 0 °C, as heavy cut. As the first step, our shortcut design method provides the values for the numbers of stages in all subsections, which are the most annoying parameters in the design of DWC, and for the liquid split ratio, resulting in a remarkable decrease in degree of freedom for design parameters and in the variance of the parameters. Another distinct feature of the shortcut method is that the solutions are easily obtained by a simple algorithm, involving the reduced iterations. The rest of the design parameters, including reflux ratio, the vapor split ratio, feed location and the side-product location, were readily determined by a sensitivity analysis in the rigorous simulation with the help of commercial software, AspenPlus®. As a reference work, the energy consumption for the distillation columns in conventional arrangements was calculated and compared to that of the DWC.

From the rigorous simulation results, the reboiler duty for the DWC was about 24% less than that of two series columns in direct sequence and about 25% less than in indirect sequence. These reduction ratios are almost close to 30%, which is popularly known as a typical value for energy saving of DWC, and, therefore, can be a positive proof that the design for the DWC in the present work, which can fractionate PME into the three more valuable products, is sufficiently effective, although a little bit of room for improvement was found. Eventually, it can be concluded that the design method for DWC in the present work is obviously practical at least, in terms of the accuracy in the design results and the applicability of the method to actual plant due to its feature of requiring less effort. However, the robustness and the validity of the design method in the present work must be further verified by further work.

ACKNOWLEDGEMENTS

We acknowledge the financial support by grants from Korea CCS R&D Center, funded by the Ministry of Education, Science and Technology of Korean government.

REFERENCES

1. P. Lv, Y. Cheng, L. Yang, Z. Yuan, H. Li and W. Luo, *Fuel Process. Technol.*, **110**, 61 (2013).
2. B. R. Moser, *In Vitro Cell. Dev. Biol. Plant*, **45**, 229 (2009).
3. G. C. Gervajio, *Bailey's industrial oil and fat products*, 6th Ed., Wiley, New Jersey, 1 (2005).
4. S. C. Smolinske, Handbook of food, drug, and cosmetic excipients, CRC Press, Boca Raton, FL, 75 (1992).
5. http://www.chemithon.com/Resources/pdfs/Surfactant.pdf (last accessed, August 2013).
6. R. O. Dunn and B. R. Moser, The biodiesel handbook, second Ed., AOCS Press, Urbana, IL, 147 (2010).
7. J. Y. Park, D. K. Kim, J. P. Lee, S. C. Park, Y. J. Kim and J. S. Lee, *Bioresour. Technol.*, **99**, 1196 (2008).
8. B. R. Moser, *Energy Fuels*, **22**, 4301 (2008).
9. T. C. Ming, N. Ramli, O. T. Lye, M. Said and Z. Kasim, *Eur. J. Lipid Sci. Technol.*, **107**, 505 (2005).
10. Y. M. Choo, S. F. Cheng, C. L. Yung, L. N. N. Harrison, A. N. Ma and B. Yusof, US Patent, 8,246,699 (2012).
11. S. Heck, V. Winterhoff, B. Gutsche, G. Fieg, U. Mueller and J. Rigal, US Patent, 7,064,223 (2006).
12. Y. M. Choo, L. N. N. Harrison, C. L. Yung, M. H. Ng, C. W. Puah, A. M. Rusnani et al., http://palmoilis.mpob.gov.my/publications/TOT/TT-428.pdf (last accessed, August 2013).
13. N. Asprion and G. Kaibel, *Chem. Eng. Process*, **49**, 139 (2010).
14. N. V. D. Long, S. H. Lee and M. Y. Lee, *Chem. Eng. Process*, **49**, 825 (2010).
15. N. V. D. Long and M. Y. Lee, *Korean J. Chem. Eng.*, **29**, 567 (2012).
16. N. V. D. Long and M. Y. Lee, *J. Chem. Eng. Japan*, **45**, 285 (2012).
17. L. Q. Minh, N. V. D. Long and M. Y. Lee, *Korean J. Chem. Eng.*, **29**, 1500 (2012).

18. S. G. Lee, N. V. D. Long and M. Y. Lee, *Ind. Eng. Chem. Res.*, **51**, 10021 (2012).
19. Y. H. Kim, M. Nakaiwa and K. S. Hwang, *Korean J. Chem. Eng.*, **19**, 383 (2002).
20. Y. H. Kim, K. S. Hwang and M. Nakaiwa, *Korean J. Chem. Eng.*, **21**, 098 (2004).
21. I. Dejanović, Lj. Matijašević and Ž. Olujić, *Chem. Eng. Process.*, **49**, 559 (2010).
22. K. T. Chu, L. Cadoret, C. C. Yu and J. D. Ward, *Ind. Eng. Chem. Res.*, **50**, 9221 (2011).
23. R. O. Dunn, Soybean - Applications and technology, InTech, 211 (2011).
24. M. E. G. Gómez, R. H. Hildige, J. J. Leahy and B. Rice, *Fuel*, **81**, 33 (2012).
25. M. J. Ramos, C. M. Fernández, A. Casas, L. Rodríguez and Á. Pérez, *Bioresour. Technol.*, **100**, 261 (2009).
26. K. A. Amminudin, R. Smith, Y. C. Thong and G. P. Towler, *Chem. Eng. Res. Des.*, **79**, 701 (2001).
27. A. I. Kakhu and J. R. Flower, *Chem. Eng. Res. Des.*, **66**, 241 (1988).
28. G. Dünnebier and C. C. Pantelides, *Ind. Eng. Chem. Res.*, **38**, 162 (1999).
29. J. A. Caballero and I. E. Grossman, *Ind. Eng. Chem. Res.*, **40**, 2260 (2001).
30. P. Wang, H. Chen, Y. Wang, L. Zhang, K. Huang and S. J. Wang, *Chem. Eng. Commun.*, **199**, 608 (2012).
31. I. J. Halvorsen and S. Skogestad, *Ind. Eng. Chem. Res.*, **42**, 605 (2003).
32. Z. Fidkowski and L. Krolikowski, *AIChE J.*, **32**, 537 (1986).
33. Z. Fidkowski and L. Krolikowski, *AIChE J.*, **33**, 643 (1987).
34. C. Triantafyllou and R. Smith, *Chem. Eng. Res. Des.*, **70**, 118 (1992).
35. Y. H. Kim, *Chem. Eng. J.*, **85**, 289 (2002).
36. N. V. D. Long and M. Y. Lee, *Comput. Chem. Eng.*, **37**, 119 (2012).
37. V. K. Sangal, V. Kumar and I. M. Mishra, *Comput. Chem. Eng.*, **40**, 33 (2012).
38. N. V. D. Long and M. Y. Lee, *Korean J. Chem. Eng.*, **30**, 286 (2013).
39. I. J. Halvorsen, PhD thesis, Department of Chemical Engineering, Norwegian University of Science and Technology, Trondheim, 352 (2001).
40. A. J. Underwood, *Chem. Eng. Prog.*, **44**, 603 (1948).
41. J. Stichlmair, *Chem. Ing. Technol.*, **60**, 747 (1988).
42. I. J. Halvorsen and S. Skogestad, *Ind. Eng. Chem. Res.*, **43**, 3994 (2004).
43. H. E. Edulgee, *Hydrocarbon Process*, **54**, 120 (1975).

APPENDIX

The appendix provides design procedures of a short-cut model proposed by Chu et al. [22]. First, the recovery of component i as top product at section 1 (β_i), defined as the fraction of i sent to the top of the pre-fractionator, is given in Eq. (A1).

$$\beta_i = D_1 X_{D1,i} / F Z_i \tag{A1}$$

where, D_j is the net molar flow rate of top product at section j, W_j is the net molar flow rate of bottom product at section j and $X_{k,i}$ is the composition of i in the stream k. β_B is a key variable for the design and will be determined for DWC to be balanced properly during the calculation of minimum vapor flow, while suitable values for β_A, β_C should be set in order that net internal flows (D_3, W_3) should not be minus value and that the specifications of side-product should be met. Then, all values for the net molar flow rates of products (D_2, S, W_4) and net internal flows (D_1, D_3, W_1, W_3), and for the composition of i in the stream k ($X_{k,i}$) can be obtained by solving the set of algebra equations simultaneously, which are mass balances as shown in Chu et al. [22], with the data in Table 3 and β_i.

As described in Chu et al. [22], the next step in the calculation, after the establishment of the component net flow model, is to estimate the minimum vapor flow rate in each column section using Underwood's method [40], which relies on the assumptions of constant molar flow rate and constant relative volatility. The calculation of minimum vapor flow rate for only section 1 is briefly described here, having been discussed by several authors [31-33] besides Chu et al. [22]. In section 1, the Underwood root is obtained from Eq. (A2) as below:

$$(1-q) = \Sigma\, \alpha_{iC} Z_i / (\alpha_{iC} - \theta),\ i=\{A, B, C\} \tag{A2}$$

which has solutions

$$\alpha_{AC} > \theta_1 > \alpha_{BC} > \theta_2 > \alpha_{CC} \tag{A3}$$

The minimum vapor flows in section 1, $V_{min,1}$, are calculated on the basis of the roots, and the larger one is chosen:

$$V_{min,1} = \Sigma\, \alpha_{iC} X_{D1,i} D_1 / (\alpha_{iC} - \theta) = \Sigma\, \alpha_{iC} \beta_i Z_i F / (\alpha_{iC} - \theta) \tag{A4}$$

$$V_{min,1} = \mathrm{Max}\{V_{min,1}(\theta_1), V_{min,1}(\theta_2)\} \tag{A5}$$

Likewise, the minimum vapor flow in the other section i, $V_{min,i}$, is calculated as described in Chu et al. [22] and the minimum vapor flow for DWC is chosen as

$$V_{min,DWC} = \mathrm{Max}\{V_{min,2}, V_{min,4} + (1-q)F\} \tag{A6}$$

As found in Eq. (A4), the minimum vapor flow calculation depends on β_B. The minimum vapor flow is constant between two special points called "beta preferred" (β_p) [41] and "beta balanced" (β_b) [42] and $V_{min,DWC}$ is minimized in this section. β_p is the value of β_B for which $V_{min,1}$ is a minimum and β_b is the value of β_B for which $V_{min,3\_1}$ is equal to $V_{min,3\_2}$ [22]. In the present study, β_b was chosen for the shortcut design, considering that the withdrawal of vapor side-product would be very rare case in actual operation of DWC. The minimum reflux ratio of DWC, $R_{min,2}$, is calculated by Eq. (A7).

$$R_{min,2} = V_{min,2} / D_2 - 1 \tag{A7}$$

In the next step, the minimum numbers of stages are calculated using the Fenske equation, which requires only the assumption of constant volatility [39]. The minimum numbers of stages for section 1, $N_{min,1}$, is calculated by Eq. (A8) as below and the largest one among three values is chosen.

$$N_{min,1} = \ln[(X_{m,D1}/X_{n,D1})(X_{n,W1}/X_{m,W1})] / \ln \alpha_{mn},\ m, n=\{A, B, C\} \tag{A8}$$

Section 2 and section 3_1 should be combined for the purpose of calculating the minimum number of stages:

$$N_{min,2} + N_{min,3\_1} = \ln[(X_{m,D2}/X_{n,D2})(X_{n,S3\_1}/X_{m,S3\_1})] / \ln \alpha_{mn},\ m, n=\{A, B\} \tag{A9}$$

Section 4 and section 3_2 should also be combined:

$$N_{min,4}+N_{min,3\_2}=\ln\left[(X_{m,S3\_2}/X_{n,S3\_2})(X_{n,W4}/X_{m,W4})\right] / \ln \alpha_{mn},\ m,\ n=\{B, C\} \quad (A10)$$

The ratio of $N_{min,2}$ to $N_{min,3\_1}$ and the ratio of $N_{min,4}$ to $N_{min,3\_2}$ are degrees of freedom and these values will be determined in the next design procedure [22].

The reflux ratio and minimum reflux ratio for each section should be defined before using the Gilliland correlation, which empirically relates the number of stages at finite reflux ratio, N, to the N_{min} and R_{min}. For section 1, 2 and 3_1, the reflux ratio, R_i, and the minimum reflux ratio, $R_{min,i}$, are defined as Eq. (A11) and (A12).

$$R_{min,i}=L_{min,i}/D_i \quad (A11)$$

$$R_i=L_i/D_i \quad (A12)$$

where $L_{min,i}$ and L_i are the minimum internal liquid flowrate and the internal liquid flowrate in the section i, respectively. The definitions for section 4 are given as Eq. (A13) and (A14).

$$R_{min,4}=L_{min,4}/(W_1-W_3) \quad (A13)$$

$$R_4=L_4/(W_1-W_3) \quad (A14)$$

The definitions for section 3_2 are shown as Eq. (A15) and (A16).

$$R_{min,3\_2}=L_{min,3\_2}/S_{3\_2} \quad (A15)$$

$$R_{3\_2}=L_{3\_2}/S_{3\_2} \quad (A16)$$

On the other hand, liquid split ratio (SL) and vapor split ratio (SV) of DWC in the present work are defined as follows:

$$SL=L_1/L_2=(L_2-L_{3\_1})/L_2 \quad (A17)$$

$$SV=\overline{V_1}/V_4=(V_4-V_{3\_2})/V_4 \quad (A18)$$

where V_i and $\overline{V_i}$ are the internal vapor flowrate for the upper part of the section i and for the lower part of the section i, respectively, as shown in Fig. 3. SL and SV are dependent on each other due to the constant mole flow assumption in shortcut design. The reflux ratios for section 1, 3_1, and 3_2 are found to depend on SL or SV from Fig. 3, Eqs. (A12) and (A16), and, consequently, the number of stages for these sections is also affected by SL or SV. Therefore, the values of SL or SV are chosen so that there are the same number of stages in section 1 and section 3 and the smallest number of stages for these sections during the design procedure.

Once R_2 is set to a certain ratio to $R_{min,2}$, e.g. $R_2=1.2R_{min,2}$, and SL or SV is assumed, the reflux ratios for all sections are calculated one by one using the above equations, and, then, the number of stages for all sections, N_i, are estimated by the Gilliland correlation [43] as shown in Eq. (A19).

$$(N_i-N_{min,i})/(N_i+1)=0.75\left[1-((R_i-R_{min,i})/(R_i+1))^{0.5688}\right] \quad (A19)$$

Then, the Kirkbride equation is used to determine the feed location for section 1:

$$(N_{1\_1}/N_{1\_2})=\left[(W_1/D_1)\,(Z_C/Z_A)\,(X_{W1,A}/X_{D1,C})^2\right]^{0.206} \quad (A20)$$

where N_{1_1}, N_{1_2} are the numbers of stages above and below feed, respectively. The ratio of N_2 to N_{3_1} and the ratio of N_{3_1} to N_4 should also be determined by the Kirkbride equation as shown in Eqs. (A21) and (A22).

$$(N_2/N_{3\_1})=\left[(S_{3\_1}/D_2)\,(X_{D1,B}/X_{D1,A})\,(X_{S3\_1,A}/X_{D2,B})^2\right]^{0.206} \quad (A21)$$

$$(N_{3\_2}/N_4)=\left[(W_4/S_{3\_2})\,(X_{W1,C}/X_{W1,B})\,(X_{W4,B}/X_{S3\_2,C})^2\right]^{0.206} \quad (A22)$$

The ratios, determined by the Kirkbride equation, are used to determine initial values of $N_{min,2}$, $N_{min,3\_1}$, $N_{min,3\_2}$, and $N_{min,4}$ and replaced with the newly updated values during iterations.